Supporting Information

Engineering of Ternary Co-Crystals Based on Differential Binding of Guest Molecules by a Tetraarylpyrene Inclusion Host

Jarugu Narasimha Moorthy,* Palani Natarajan and P. Venugopalan

†Department of Chemistry, Indian Institute of Technology, Kanpur 208 016, INDIA
Department of Chemistry, Panjab University, Chandigarh 160014, INDIA

Table of Contents

EXPERIMENTAL SECTION

Anhyd tetrahydrofuran (THF) was freshly distilled over sodium prior to use. All other solvents were distilled prior to use. The progress of reactions was monitored by analytical thin layer chromatography (TLC) using aluminum sheets pre-coated with silica gel. Column chromatography was conducted with silica gel (60-120 μm mesh). ^{1}H and ^{13}C NMR spectra were recorded on 400 and 500 MHz spectrometers using deuterated solvents. TGA and DSC measurements were carried out at a heating rate of 10 ^{o}C/min under nitrogen gas atmosphere. Commercial chemicals were used as received. X-ray powder patterns were recorded on a Rigaku X-ray diffractometer.

Synthesis of Tetararylpyrene TP

The synthesis of tetrarylpyrene **TP** involved 4-fold Suzuki coupling of 1,3,6,8-tetrabromopyrene with 2,6-dimethyl-4-methoxyphenylboronic acid using $Pd(PPh_3)_4$ as a catalyst, and has been previously reported by us.[1]

General Procedure for Synthesis of Ternary Inclusion Compounds

A 1:2 mixture of host **TP** and solid guest were dissolved in a minimum amount of appropriate liquid guest. Slow evaporation of the resultant solution over a period of two weeks led to colorless crystals quantitatively. When both guests were liquida, the low boiling guest was used in excess for crystallization. The crystal structures of ternary inclusion compounds of **TP** with guest molecules in Chart 1 were determined by X-ray crystallography. The details of crystal data and structure determination are given in Table 1. In most cases, the guest inclusion was independently established by TGA, ^{1}H NMR spectroscopy GC and PXRD analyses.

X-Ray Crystal Structure Determination. A good quality crystal in each case was mounted in a glass capillary, cooled to 100/298 K, and the intensity data were collected on a Bruker Nonius SMART APEX CCD detector system with Mo-sealed Siemens ceramic diffraction tube (λ = 0.71073) and a highly oriented graphite monochromator operating at 50 kV and 30 mA. The data were collected on a hemisphere mode and processed with Bruker SAINTPLUS. Empirical absorption correction was made using Bruker SADABS. The structure was solved in each case by Direct Methods using SHELXTL package and refined by full matrix least-squares method based on F^2 using SHELX97 program.[2] All the non-hydrogen atoms were refined anisotropically. The hydrogen atoms were included in the ideal positions with fixed isotropic U values and were riding with their respective non-hydrogen atoms. The experimental details of crystal data, intensity measurements, structure solution and refinements are presented in Table 1.

References

1 (a) J. N. Moorthy, P. Natarajan, P. Venkatakrishnan, D-F. Huang, T. J. Chow, *Org. Lett*. **2007**, *9*, 5215.

2 SHELX97 Program for the Refinement and Solution of Crystal Structures; G. M. Sheldrick, University of Gottingen: Gottingen, Germany, 1997.

Table 1. The Crystal data for the Ternary Inclusion Compounds of **TP**.

Identification code	**TP-PO**	**TP-PC**	**TP-MC**	**TP-PB**
Empirical formula	$C_{68}H_{71}O_4$	$C_{69}H_{61}Cl_3O_4$	$C_{62}H_{63}Cl_3O_4$	$C_{74}H_{66}O_4$
Formula weight	952.25	1060.53	978.47	1019.27
Temperature (K)	100(2)	100(2)	100(2)	100(2)
Wavelength (Å)	0.71073	0.71073	0.71073	0.71073
Crystal system	Monoclinic	Monoclinic	Monoclinic	Monoclinic
Space group	$P2_1/n$ (no. 14)	$P2_1/c$ (no. 14)	$P2_1/n$ (no. 14)	$P2_1/c$ (no. 14)
a (Å)	18.140(3)	25.857(5)	13.594(4)	14.678(7)
b (Å)	15.209(2)	15.118(3)	15.769(4)	14.855(5)
c (Å)	19.375(3)	13.916(2)	24.726(7)	14.259(1)
α (deg)	90.00	90.00	90.00	90.00
β (deg)	96.41	93.23	99.67	118.63(2)
γ (deg)	90.00	90.00	90.00	90.00
Volume ($Å^3$)	5312.1(14)	5431.1(16)	5225.0(2)	2728.3(5)
Z	4	4	4	2
Calculated density (mg/m^3)	1.191	1.297	1.244	1.241
Absorption coefficient (mm^{-1})	0.072	0.221	0.223	0.075
F(000)	2044	2232	2072	1084
Theta range for data collection (°)	2.11 to 25.50	2.07 to 25.00	1.99 to 26.00	2.09 to 25.00
Scan type	2θ–θ	2θ–θ	2θ–θ	2θ–θ
Index ranges	-21<=h<=20, -13<=k<=18, -23<=l<=22	-21<=h<=30, -17<=k<=17, -14<=l<=16	-14<=h<=16, -18<=k<=19, -30<=l<=30	-17<=h<=17, -17<=k<=12, -14<=l<=16
Reflections collected	27714	27548	28710	13867
Independent reflections	9811 [R(int) = 0.0746]	9512 [R(int) = 0.0708]	10216 [R(int) = 0.0745]	4780 [R(int) = 0.0495]
Refinement method	Full-matrix least-squares on F^2	Full-matrix least-squares on F^2	Full-matrix least-squares on F^2	Full-matrix least-squares on F^2
Data/restraints/parameters	9811/20/695	9512/0/685	10216/0/637	4780/0/352
Goodness-of-fit on F^2	1.053	1.060	1.036	1.028
Final R indices [I>2sigma(I)]	$R_1 = 0.0684$, $wR_2 = 0.1571$	$R_1 = 0.0699$, $wR_2 = 0.1568$	$R_1 = 0.0598$, $wR_2 = 0.1302$	$R_1 = 0.0550$, $wR_2 = 0.1219$
R indices (all data)	$R_1 = 0.1182$, $wR_2 = 0.1787$	$R_1 = 0.1147$, $wR_2 = 0.1791$	$R_1 = 0.0987$, $wR_2 = 0.1515$	$R_1 = 0.0888$, $wR_2 = 0.1355$
Largest diff. peak and hole (e. $Å^{-3}$)	0.300 and -0.273	0.243 and -0.172	0.356 and -0.410	0.244 and -0.180
Host:Guest	**1 : 0.5 : 1**	**1 : 1 : 1**	**1 :1 : 1**	**1 :1 : 1**

Identification code	**TP-NP**	**TP-FB**	**TP-AO**	**TP-BM**
Empirical formula	$C_{70}H_{64}O_4$	$C_{71}H_{66}O_4$	$C_{67}H_{71}O_4$	$C_{63}H_{65}NO_6$
Formula weight	969.21	983.24	940.24	932.16
Temperature (K)	100(2)	100(2)	100(2)	293(2)
Wavelength (Å)	0.71073	0.71073	0.71073	0.71073
Crystal system	Monoclinic	Monoclinic	Monoclinic	Orthorhombic
Space group	$P2_1/n$ (no. 14)	$P2_1/n$ (no. 14)	$P2_1/n$ (no. 14)	$Pca2_1$ (no. 29)
a (Å)	14.001(5)	14.433(7)	18.050(6)	14.829(4)
b (Å)	14.840(5)	14.189(4)	15.120(5)	15.582(5)
c (Å)	14.493(5)	14.865(6)	19.430(6)	23.732(7)
α (deg)	90.00	90.00	90.00	90.00
β (deg)	117.09	118.02(2)	98.44(3)	90.00
γ (deg)	90.00	90.00	90.00	90.00
Volume ($Å^3$)	2681.2(17)	2687.0(5)	5245.0(3)	5484.0(3)
Z	2	2	4	4
Calculated density (mg/m^3)	1.201	1.215	1.191	1.129
Absorption coefficient (mm^{-1})	0.073	0.074	0.072	0.071
F(000)	1032	1048	2020	1992
Theta range for data collection (°)	2.09 to 25.00	2.11 to 25.00	2.14 to 25.00	2.08 to 25.00
Scan type	$2\theta–\theta$	$2\theta–\theta$	$2\theta–\theta$	$2\theta–\theta$
Index ranges	-16<=h<=15, -14<=k<=17, -14<=l<=17	-17<=h<=14, -16<=k<=14, -14<=l<=17	-21<=h<=16, -16<=k<=17, -23<=l<=20	-15<=h<=17, -18<=k<=17, -27<=l<=28
Reflections collected	13498	13616	26547	27514
Independent reflections	4694 [R(int) = 0.0497]	4674 [R(int) = 0.0505]	9162 [R(int) = 0.0510]	9470 [R(int) = 0.0681]
Refinement method	Full-matrix least-squares on F^2	Full-matrix least-squares on F^2	Full-matrix least-squares on F^2	Full-matrix least-squares on F^2
Data/restraints/parameters	4694/2/369	4674/42/397	9162/32/714	9470/207/705
Goodness-of-fit on F^2	1.042	1.025	1.058	1.056
Final R indices [I>2sigma(I)]	$R_1 = 0.0571$, $wR_2 = 0.1452$	$R_1 = 0.0569$, $wR_2 = 0.1279$	$R_1 = 0.0673$, $wR_2 = 0.1645$	$R_1 = 0.0944$, $wR_2 = 0.2098$
R indices (all data)	$R_1 = 0.0768$, $wR_2 = 0.1589$	$R_1 = 0.0903$, $wR_2 = 0.1432$	$R_1 = 0.1003$, $wR_2 = 0.1827$	$R_1 = 0.1601$, $wR_2 = 0.2424$
Largest diff. peak and hole (e. $Å^{-3}$)	0.305 and -0.232	0.221 and -0.212	0.643 and -0.410	0.515 and -0.245
Host:Guest	**1 : 1 : 1**	**1 : 1 : 1**	**1 : 0.5 : 1**	**1 : 1 : 1**

Table 2. The Calculated Angles (deg) Between the Mean Planes of the Aryl Rings (Involving Carbon Atoms of the Phenyl Ring) the Central Pyrene Ring (All 16 Carbons), and the Guest Accessible Volume in all Structures of **TP** with Guest Molecules.

No	code	angles (deg)		V (%)	No	code	angles (deg)		V (%)
1	**TP-PO**	77.24	89.88	29.6	5	**TP-NP**	84.23	86.28	31.7
		84.02	87.03						
2	**TP-PC**	79.13	87.04	31.9	6	**TP-FB**	86.09	88.60	31.9
		84.63	86.73						
3	**TP-MC**	83.07	87.16	30.4	7	**TP-AO**	81.92	88.76	28.4
		85.11	87.31				82.43	83.92	
4	**TP-PB**	82.92	86.42	32.1	8	**TP-BM**	78.61	82.48	33.0
							81.39	84.83	

V = guest-accessible volume

Table 3. The Ranges of Weak C─H···O and C─H···л Hydrogen Bond Distances and л···л Interaction Distances Noticed From the Ternary Inclusion Compounds of Host **TP** with Guest Molecules

code	C─H···O *d*/Å	C─H···л *d*/Å	л···л *d*/Å
TP-PO	2.63 – 2.77	2.78 – 3.00	3.78 – 3.80
TP-PC	2.79 – 2.87	2.88 – 3.07	3.79 – 3.81
TP-MC	2.32 – 2.78	2.89 – 3.08	–
TP-PB	–	2.77 – 2.98	3.76 – 3.78
TP-NP	2.55 – 2.76	2.81 – 3.09	–
TP-FB	2.67 – 2.89	2.91 – 3.06	–
TP-AO	2.63 – 2.75	2.92 – 3.01	–
TP-BM	2.55 – 2.79	2.98 – 3.07	–

Table 4. Observed Inter-molecular Interactions in all the Ternary Inclusion Compounds of Host **TP** with Guest Molecules

Identification code	Interaction	d/Å	θ/deg
TP-PO	C_{51}–H···O_3	2.777	120.78
	C_{33}–H···O_1	2.627	109.67
TP-PC	C_{51}–H···O_3	2.798	133.91
TP-MC	C_{42}–H···O_1	2.773	136.29
	C_{59}–H···O_2	2.689	144.03
	C_{43}–H···O_1	2.648	151.02
	C_{61}–H···O_2	2.600	162.22
	C_{52}–H···O_3	2.542	148.70
	C_{62}–H···O_4	2.316	152.10
TP-NP	C_{26}–H···O_2	2.764	146.09
	C_{26}–H···O_1	2.551	124.94
	C_{35}–H···O_2	2.619	145.09
	C_{39}–H···O_1	2.445	131.46
TP-FB	C_{26}–H···O_1	2.889	108.48
	C_{26}–H···O_1	2.873	109.56
	C_{26}–H···O_2	2.666	109.41
TP-AO	C_{43}–H···O_4	2.626	169.94
	C_{60}–H···O_3	2.754	168.81
TP-MB	C_{52}–H···O_1	2.797	133.27
	C_{32}–H···O_5	2.546	114.99

Chart 1. Molecular Sructures of the Guests Used for Inclusion with the Host **TP**

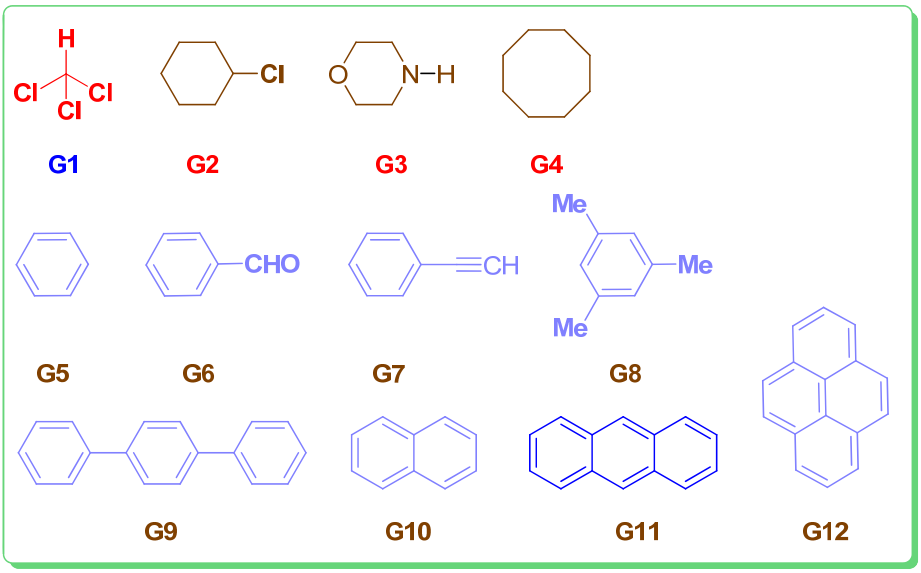

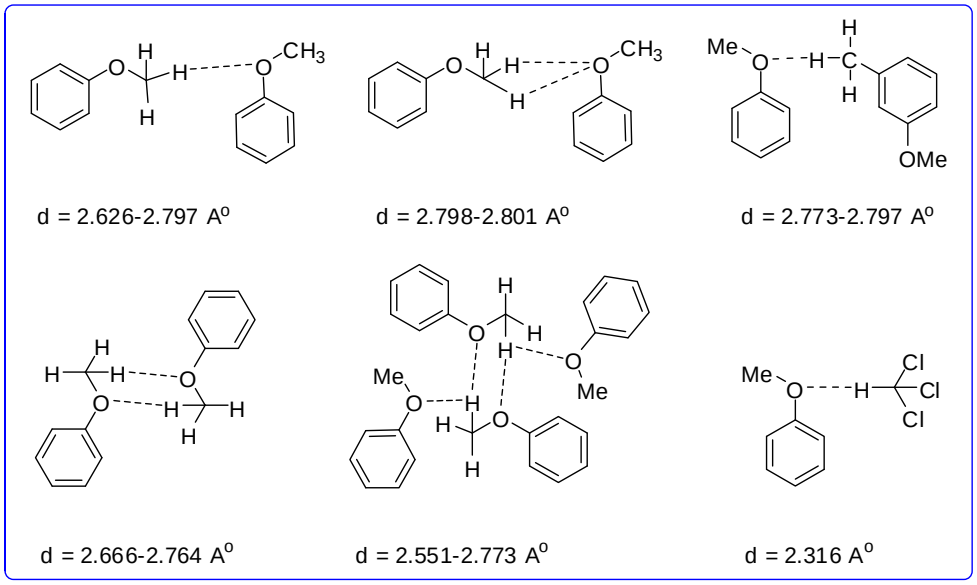

Figure S1. Weak C–H···O hydrogen bonds that are found in the crystal structures of the ternary inclusion compounds of **TP** with guest molecules.

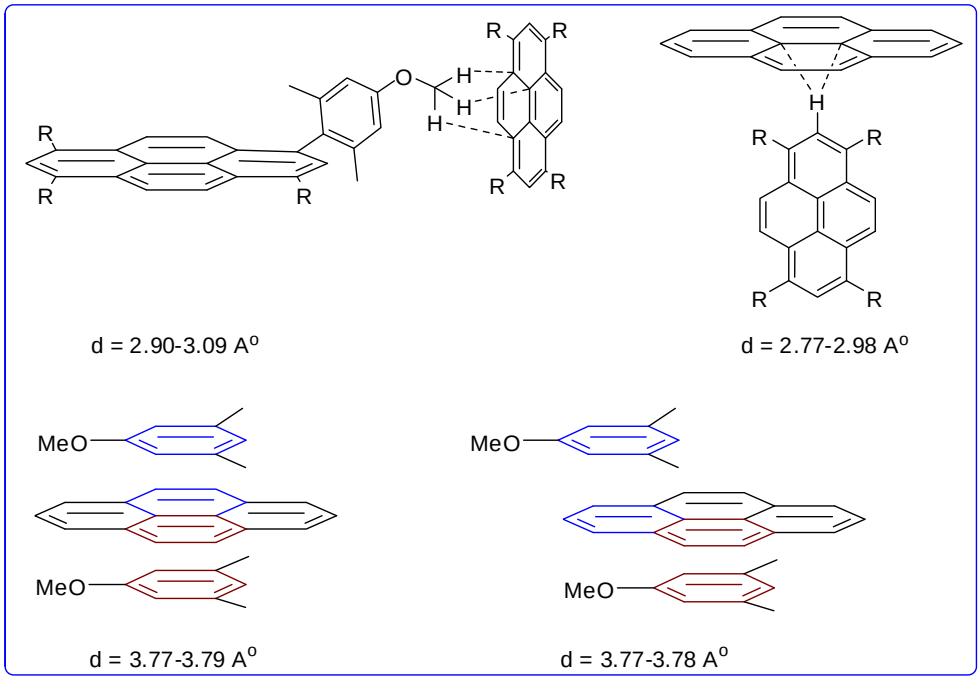

Figure S2. The edge-to-face C–H···π interactions and face-to-face π–π stacking observed between host-host and host-guest molecules in **TP** clathrates.

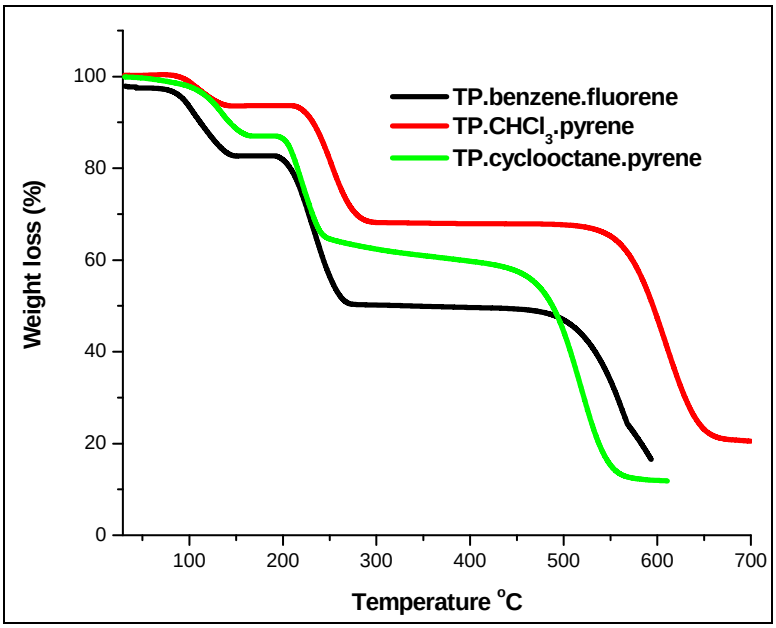

Figure S3. The TGA plots for the ternary inclusion compounds of **TP** with guest molecules pyrene+$CHCl_3$ (red), pyrene+cyclooctane (green) and fluorene+benzene (black).

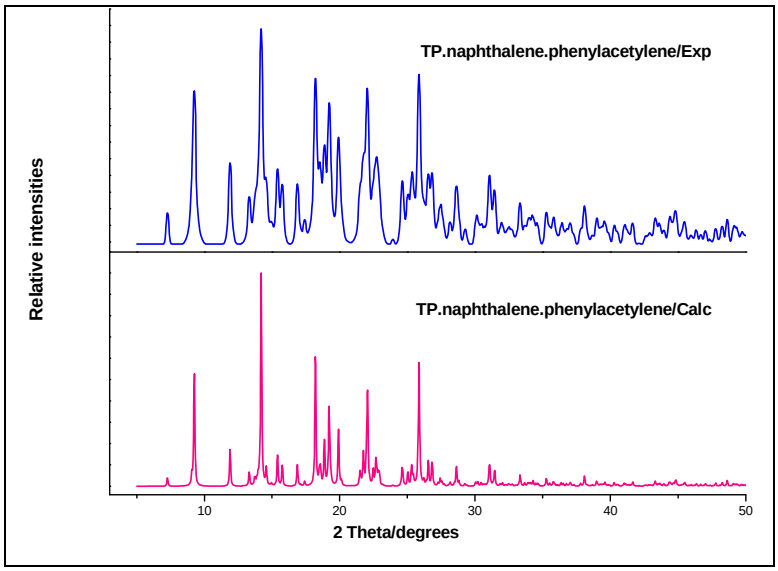

Figure S4. Top: powder X-ray diffraction pattern for the ternary inclusion compound of **TP**•naphthalene•phenylacetylene. Bottom: simulated PXRD pattern based on single crystal X-ray structure determination.

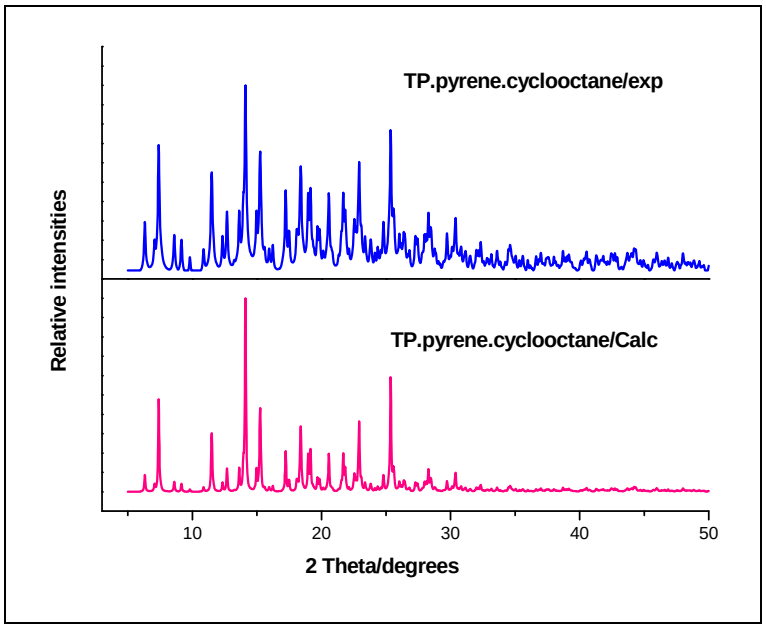

Figure S5. Top: powder X-ray diffraction pattern for the ternary inclusion compound of **TP**•pyrene•cyclooctane. Bottom: simulated PXRD pattern based on single crystal X-ray structure determination.

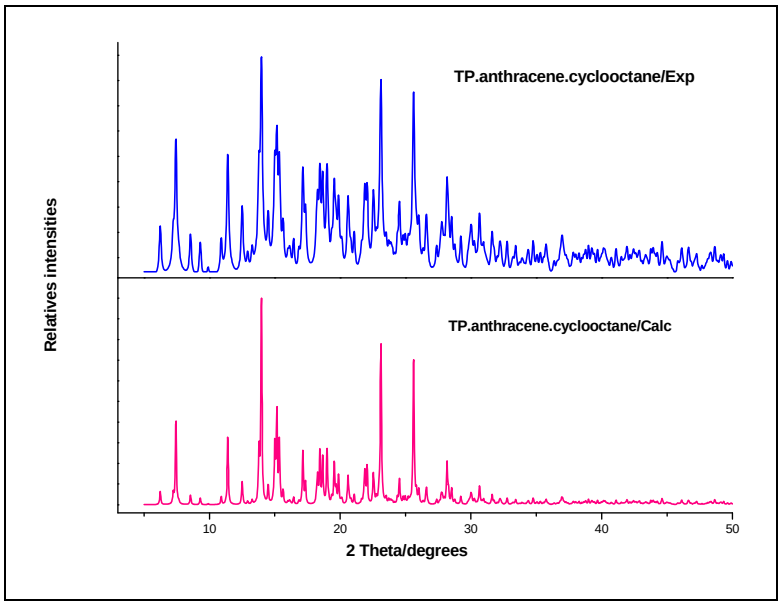

Figure S6. Top: powder X-ray diffraction pattern for the ternary inclusion compound of **TP**•anthracene•cyclooctane. Bottom: simulated PXRD pattern based on single crystal X-ray structure determination.

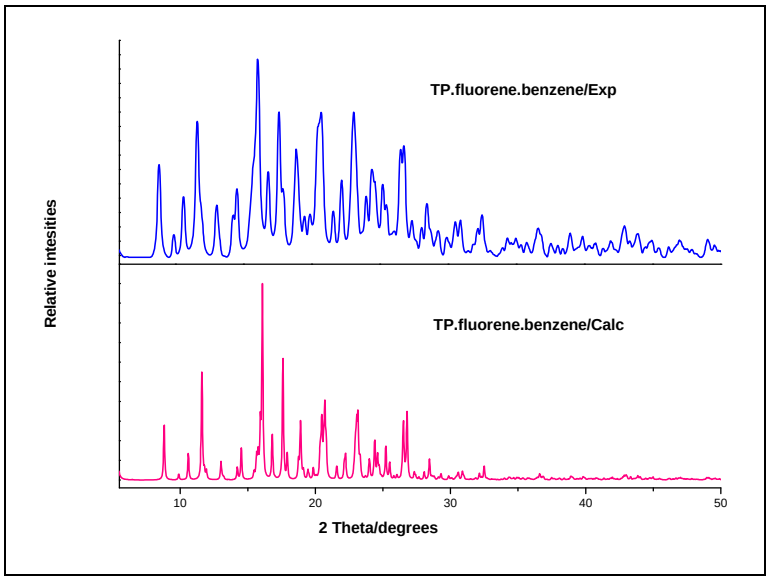

Figure S7. Top: powder X-ray diffraction pattern for the ternary inclusion compound of **TP**•fluorene•benzene. Bottom: simulated PXRD pattern based on single crystal X-ray structure determination.

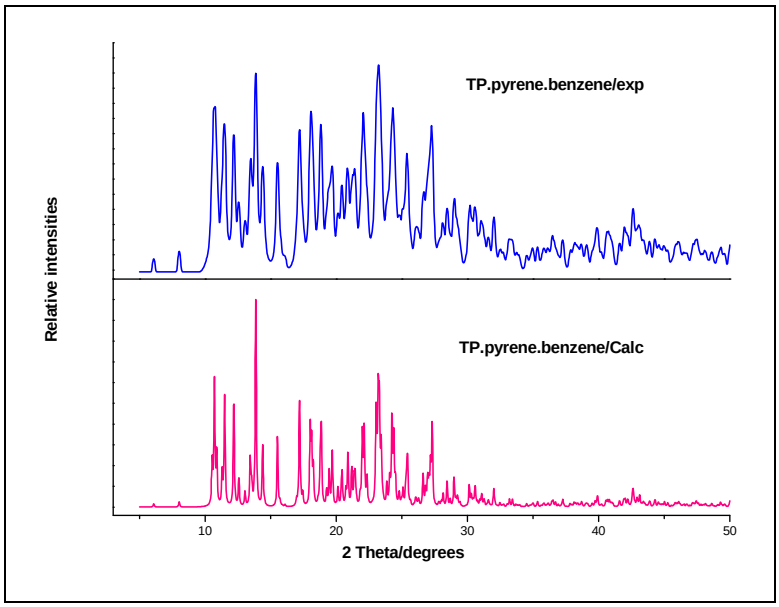

Figure S8. Top: powder X-ray diffraction pattern for the ternary inclusion compound of **TP**•pyrene•benzene. Bottom: simulated PXRD pattern based on single crystal X-ray structure determination.

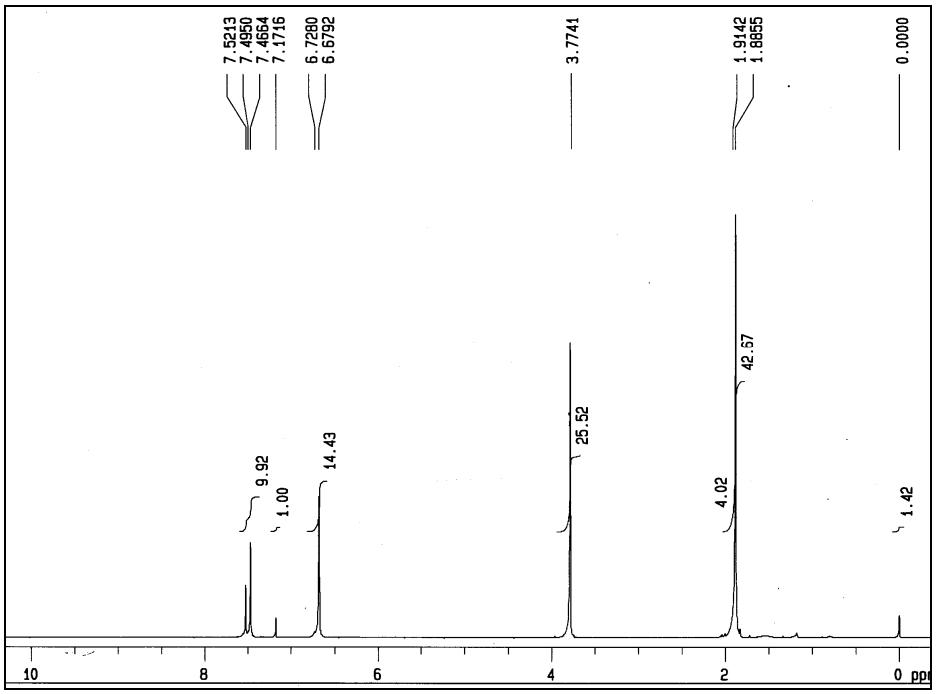

Figure S9. ^{1}H NMR spectrum of the host **TP** in $CDCl_3$.

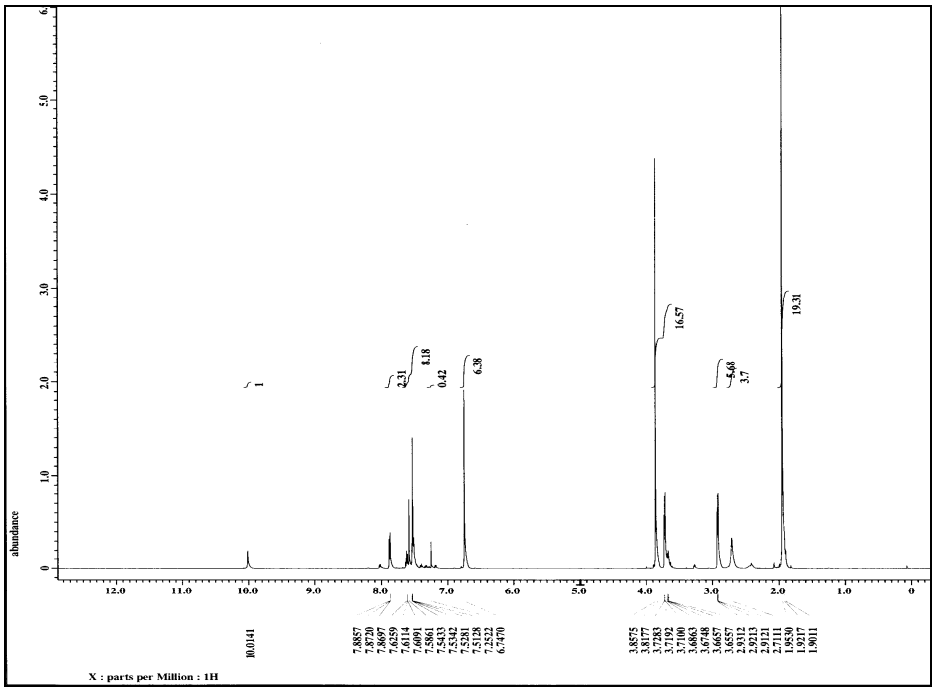

Figure S10. ^{1}H NMR spectrum for the ternary inclusion compound of **TP**•benzaldehyde•morpholine in $CDCl_3$.

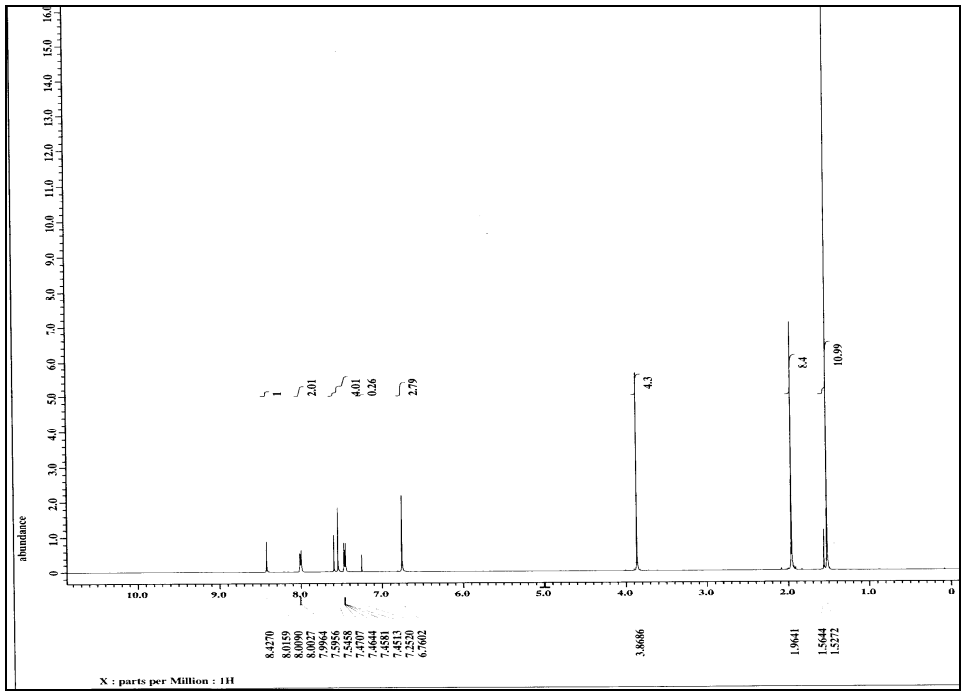

Figure S11. ^{1}H NMR spectum for the ternary inclusion compound of **TP**•antheracene•cyclooctane in $CDCl_3$

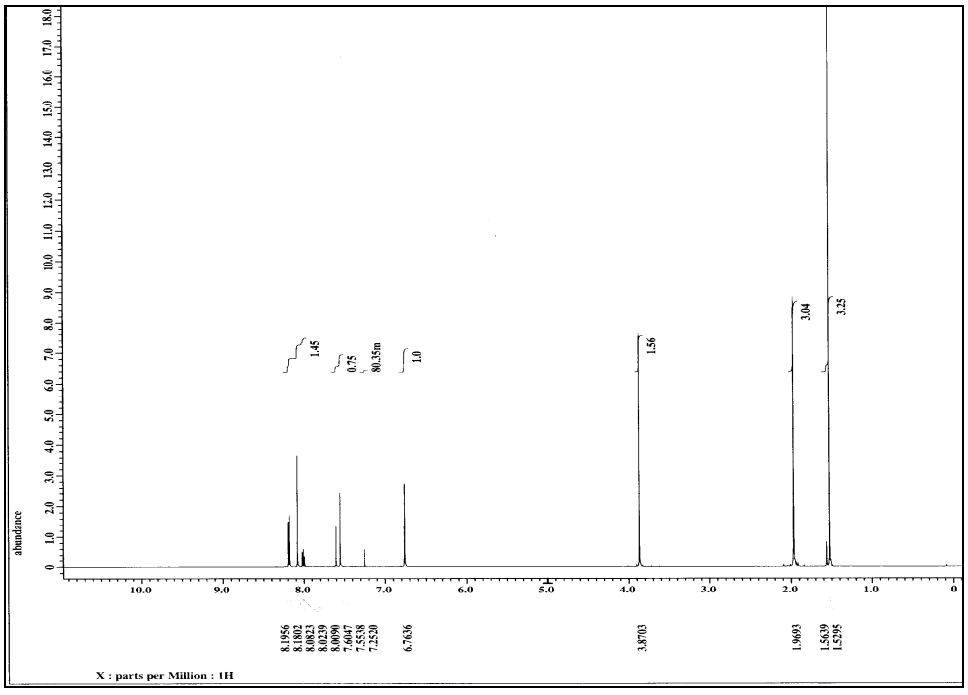

Figure S12. ^{1}H NMR spectrum for the ternary inclusion compound of **TP**•pyrene•cyclooctane in $CDCl_3$.

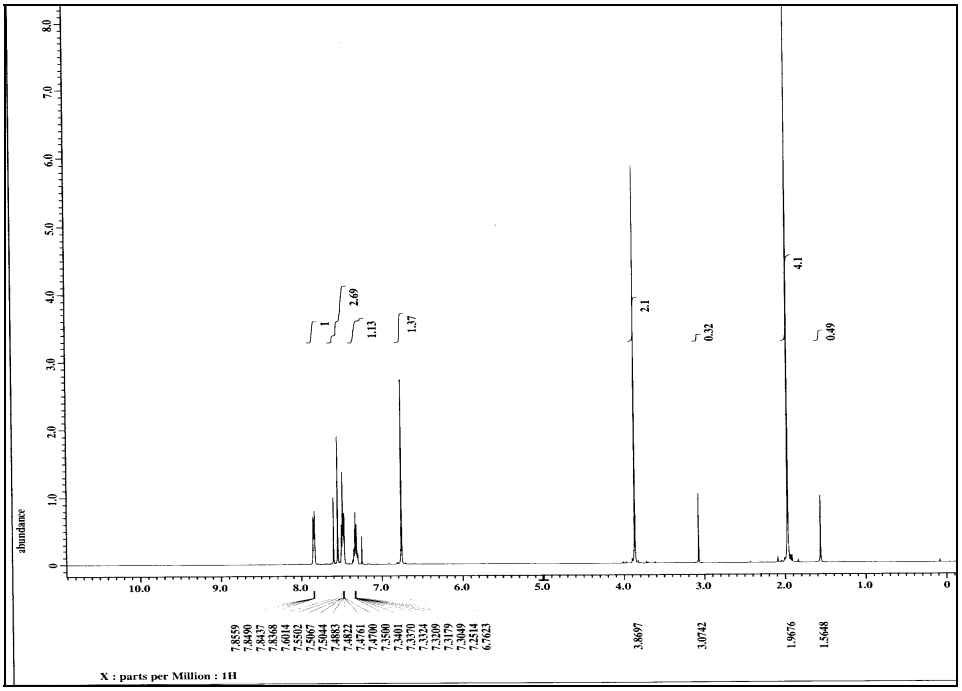

Figure S13. ^{1}H NMR spectrum for the ternary inclusion compound of **TP**•naphthalene•phenylacetylene in $CDCl_3$.

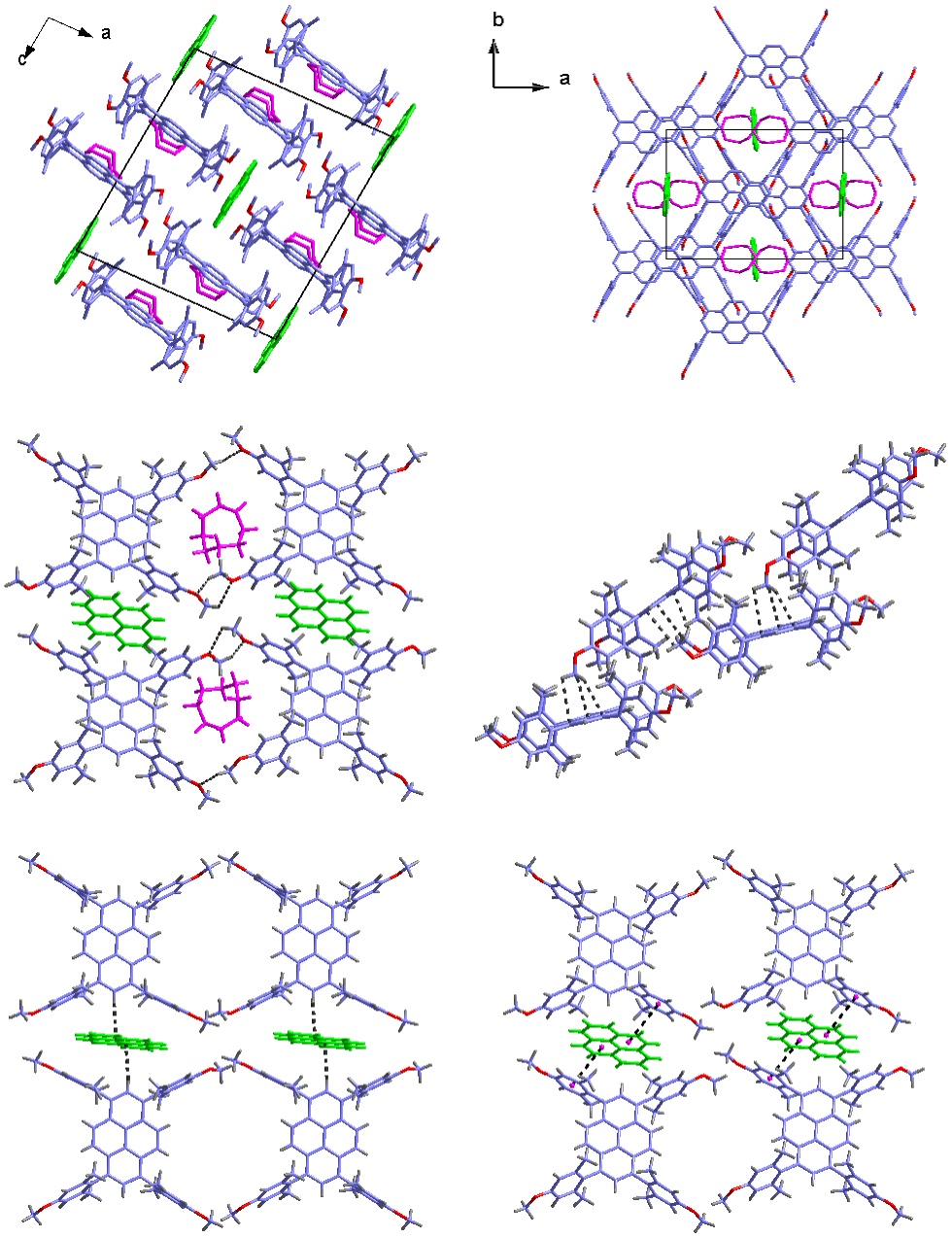

Figure S14. The crystal packing of the inclusion compound **TP**•pyrene•cyclooctane down b- and c-axes (top), the host molecules connected via both C–H···O and C–H···л hydrogen bonds (middle) and observed C–H···л and π···π hydrogen bonds between the host and guest molecules (bottom).

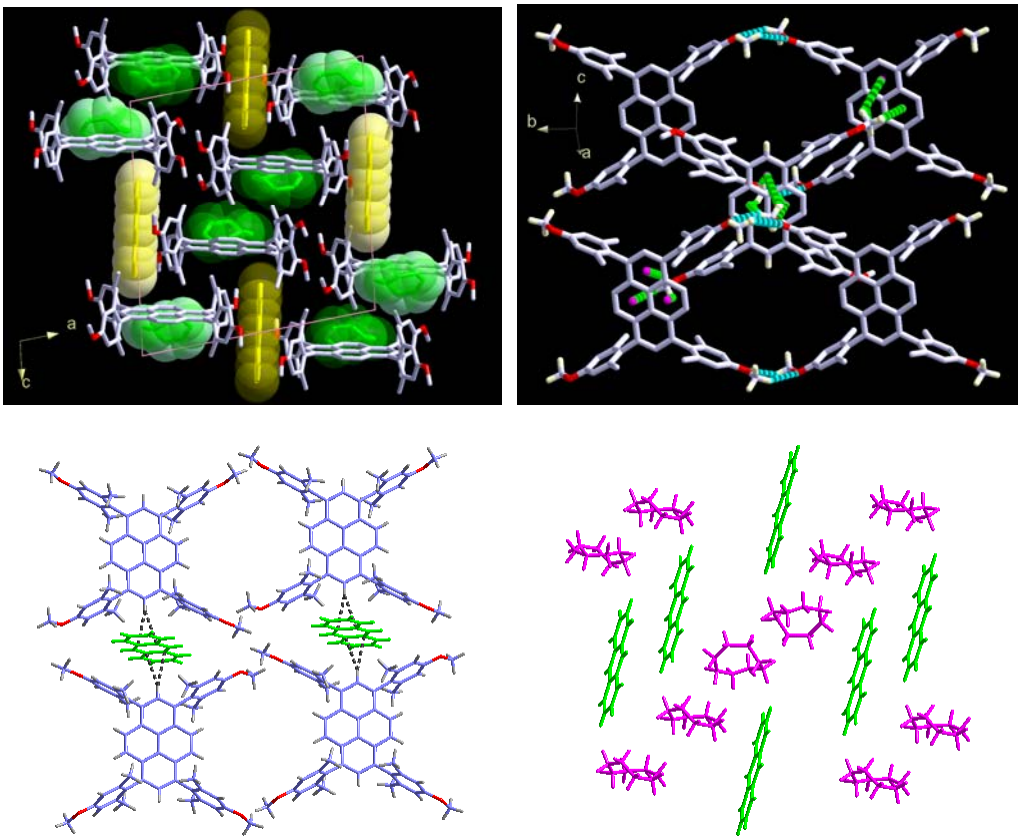

Figure S15. The crystal packing of the inclusion compound **TP**•antheracene•cyclooctane down b-axis (left). The host molecules connected via both C–H···O and C–H···л interaction (right) as in **TP-PO**.

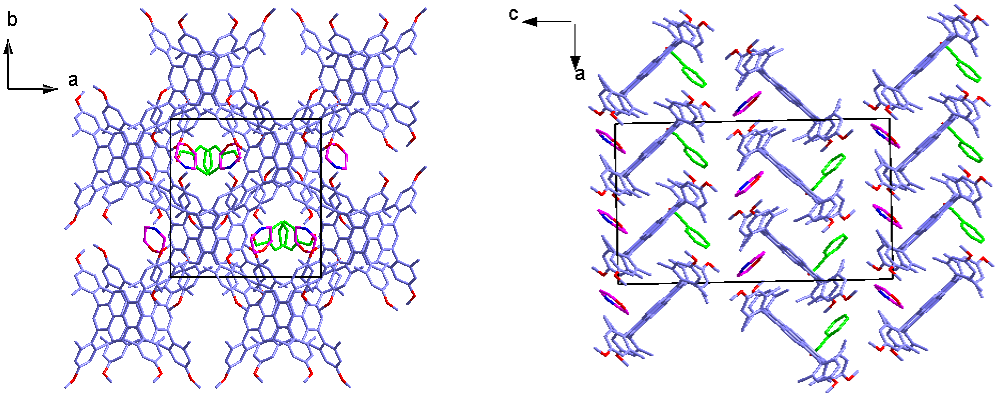

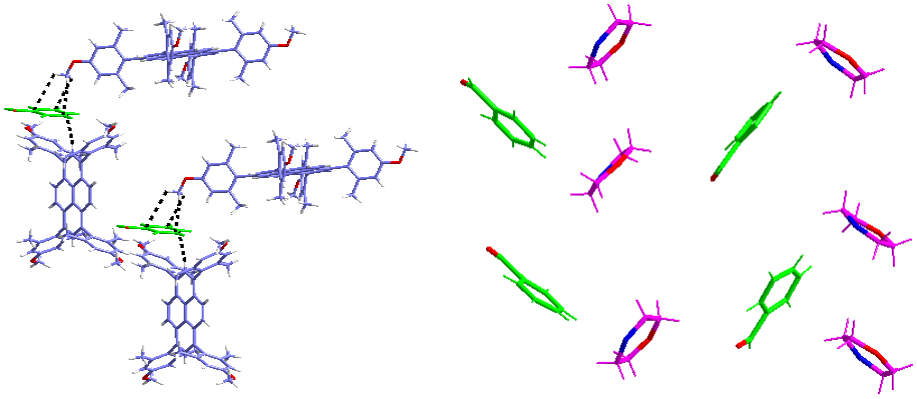

Figure S16. The crystal packing of the inclusion compound **TP**•benzaldehyde•morpholine down b-axis (left). The arrangement of host molecule alone down c-axis is shown in right.

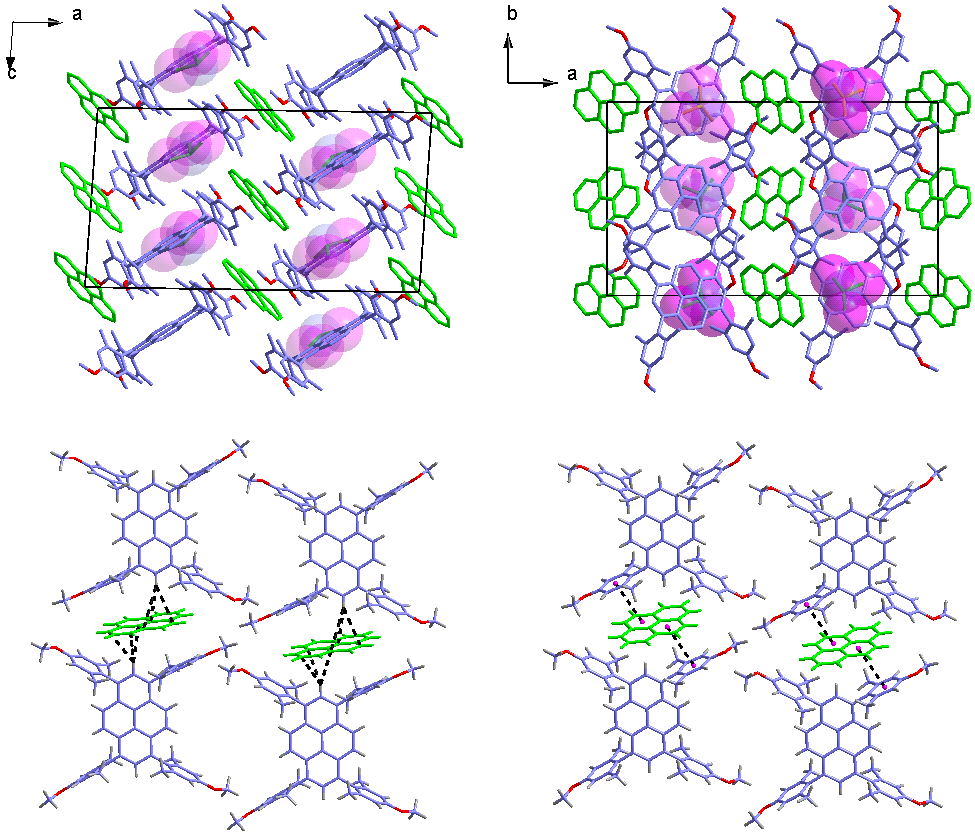

Figure S17. The crystal packing of **TP**•pyrene•$CHCl_3$, notice that the host and guest molecules are stabilized by C–H···л (left). The host also interacts via C–H···O hydrogen bond (right).

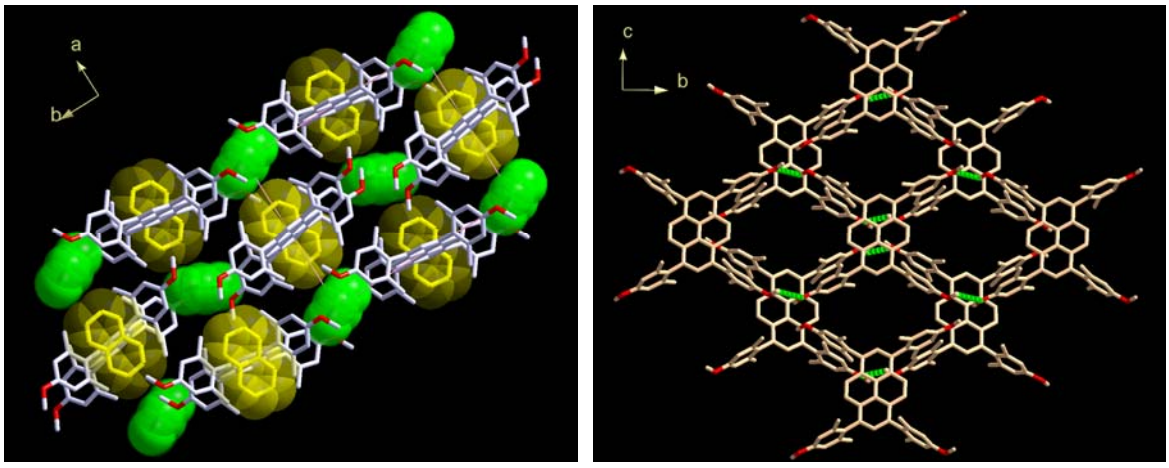

Figure S18. The molecular structure of **TP**•naphthalene•phenylacetylene down c-axis (left), notice that the host molecules are connected via C–H···O interactions (right).

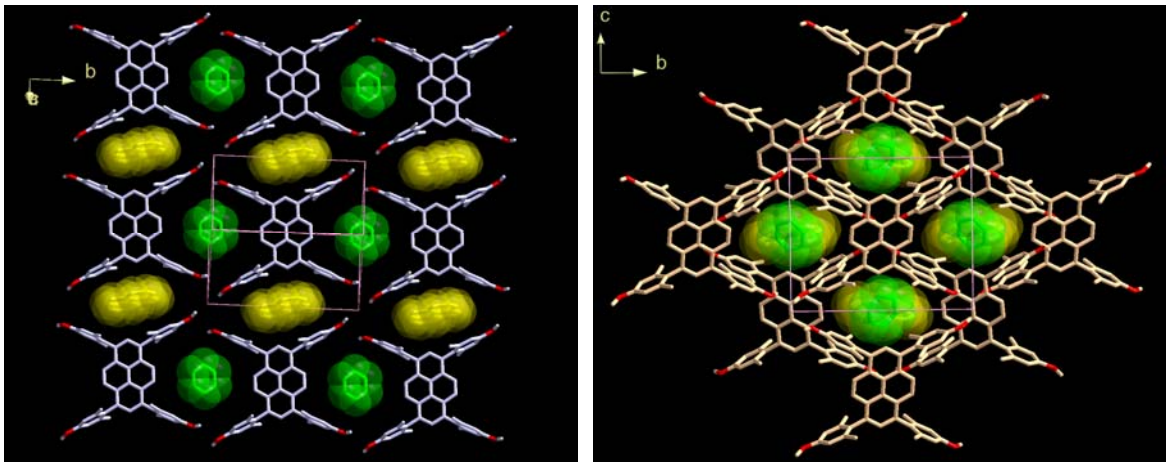

Figure S19. The molecular structure of **TP**•pyrene•benzene down c- (left) and a-axes (right). Notice that the larger size pyrene and small size benzene are bound in trough and concave domains of TP, respectively.

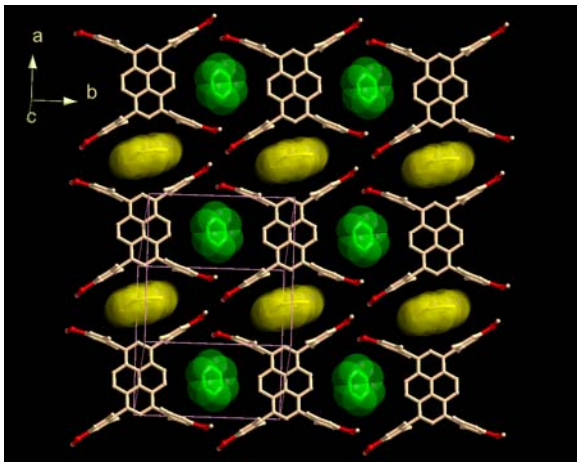

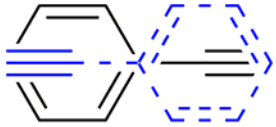

phenylacetylene

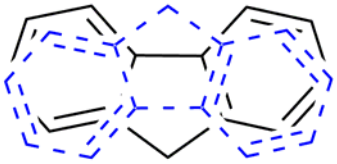

fluorene

Figure S20. The molecular structure of **TP**•fluorene•benzene down c-axis (left), notice that the larger size fluorene and small size benzene are found in trough and concave domains of **TP**, respectively. Typical modes of disorder observed in the crystal structures of the inclusion compounds **TP** with guest phenylacetylene and fluorene shown in right.